Applied Remote Sensing and Analysis

November 4, 2013

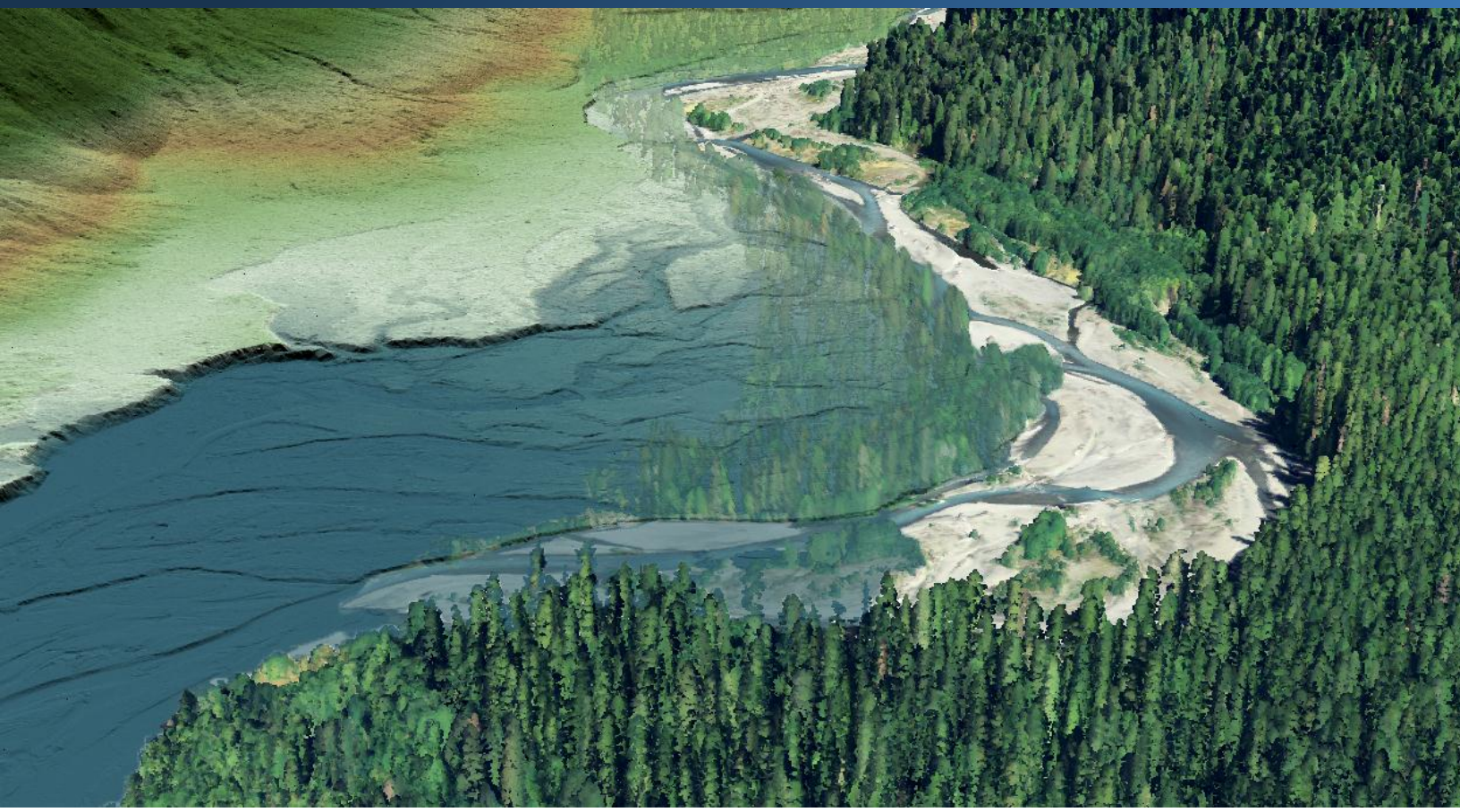

Hoh River LiDAR – Delivery 2

Technical Data Report

Steve Allison
Hoh Tribal Natural Resources
2483 Lower Hoh Rd.
Forks, WA 98331
PH: 360.374.5404

Diana Martinez
PSRC
1011 Western Ave.
Suite 500
Seattle, WA 98104
PH: 206.971.3052

WSI - Corvallis Office
517 SW 2nd St.
Suite 400
Corvallis, OR 97333
PH: 541-752-1204

TABLE OF CONTENTS

Cover Photo: View looking southwest at the Hoh River near the Hoh Rain Forest Center. Image created from gridded ground-classified LiDAR points colored by elevation partially overlaid with the LIDAR point cloud with RGB values assigned with 2011 NAIP imagery.

INTRODUCTION

View of the Hoh River on the Olympic Peninsula showing the glacial fed river and forested hillslopes in the distance.

In December 2011, WSI (Watershed Sciences, Inc.) was contracted by the Puget Sound LiDAR Consortium and the Hoh Tribe to collect Light Detection and Ranging (LiDAR) data for the Hoh River Watershed on the Olympic Peninsula of northwest Washington. Data were collected to aid the Hoh Tribe in assessing the topographic and geophysical properties of the study area to support natural resource and watershed management programs.

This report accompanies the second delivery of LiDAR data covering the upper watershed and documents data acquisition procedures, processing methods, and results of all accuracy assessments. Delivery 1 encompassed the lower watershed and was delivered June 29, 2012. Project specifics are shown in Table 1, the project extent can be seen in Figure 1, and a complete list of contracted deliverables can be found in Table 2.

Table 1: Acquisition dates, acreages, and data types collected on the Hoh River site

Project Site	Contracted Acres	Buffered Acres	Acquisition Dates	Delivery Date	Data Type
Lower Hoh (Delivery 1)	167,037	115,290	4/14-15/2012 4/17/2013 4/19-21/2013	6/29/2012	LiDAR
Upper Hoh (Delivery 2)		56,662	10/6-7/2012 10/10/2012 3/31/2013 4/1/2013 6/29-30/2013 7/24/2013	8/30/2013	

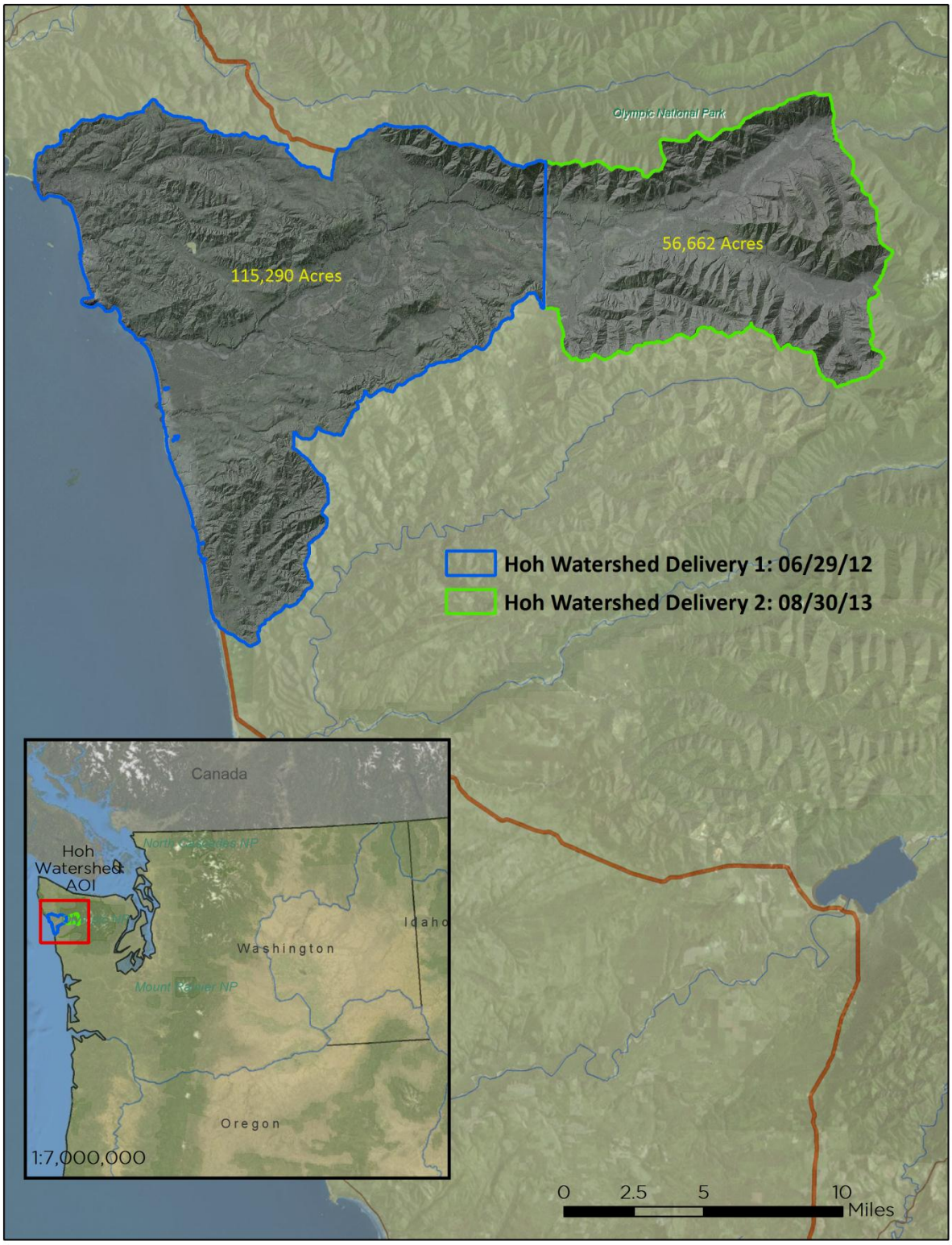

Figure 1: Location map of the Hoh River site in northwest Washington

Table 2: Products delivered to PSRC and the Hoh Tribe for the Hoh River site

Hoh River Products Projection: Washington State Plane South Horizontal Datum: NAD83 (1991 HARN) Vertical Datum: NAVD88 (GEOID03) Units: U.S. Survey Feet	
LAS Files	LAS v 1.2 • All Returns ASCII Text Files (*.txt) • All Returns • Ground Returns
Rasters	3.0-foot ESRI Grids • Bare Earth Model • Hydroflattened Bare Earth Model • Highest Hit Model • Vegetation Model • Normalized Vegetation Model 1.5-foot GeoTiffs • Intensity Images
Vectors	Shapefiles (*.shp) • Site Boundary • LiDAR Index • DEM/DSM Index • 2-foot contours • Hydrolines • Stream Network • Building & Building Footprints • RTK Ground Checkpoints • Basestation Locations ASCII Text Files (*.txt) • Smooth Best Estimate Trajectory (SBETs)

WSI Cessna Caravan

Planning

In preparation for data collection, WSI reviewed the project area using Google Earth, and flightlines were developed using a combination of specialized software. Careful planning by acquisition staff entailed adapting the pulse rate, flight altitude, scan angle, and ground speed to ensure complete coverage of the LiDAR study area at the target point density of ≥8 pulses per square meter (0.74 pulses/square foot). Efforts are taken to optimize flight paths by minimizing flight times while meeting all accuracy specifications.

Factors such as satellite constellation availability and weather windows must be considered during the planning stage. Any weather hazards or conditions affecting the flight were continuously monitored due to their potential impact on the daily success of airborne and ground operations. In addition, a variety of logistical considerations required review including private property access, potential air space restrictions, and availability of company resources (both staff and equipment).

LiDAR acquisition for the Hoh watershed was conducted during 'no snow' conditions, with emphasis on leaf-off at lower elevations where possible. In order to comply with these conditions, WSI acquired the project in phases. Beginning in April of 2012, WSI acquired all low elevation areas up to the snow line (Delivery 1). WSI visited the project site four more times through July 2013, collecting data in areas that met acquisition conditions until complete coverage was obtained.

Ground Survey

Ground survey data are used to geospatially correct the aircraft positional coordinate data and to perform quality assurance checks on final LiDAR data. Ground surveys, including monumentation and ground check points, are conducted to support the airborne acquisition process.

Monumentation

The spatial configuration of ground survey monuments provided redundant control within 13 nautical miles of the mission areas for LiDAR flights. Monuments were also used for collection of ground control points using RTK survey techniques (see **RTK** below).

Monument locations were selected with consideration for satellite visibility, field crew safety, and optimal location for RTK coverage. WSI utilized on existing monument (USDOT_MINNIE) and established 6 new monuments for the Hoh River project (Table 3, Figure 2). New monumentation was set using 5/8”x30” rebar topped with stamped 2" aluminum caps. WSI’s professional land surveyor, Chris Yotter-Brown (WA PLS# 46328 LS) oversaw and certified the establishment of all monuments.

Table 3: Monuments established for the Hoh River acquisition. Coordinates are on the NAD83 (1991 HARN) datum

Monument ID	Latitude	Longitude	Ellipsoid (meters)
HOH_01	47 43 01.50646	124 17 15.30733	145.674
HOH_02	47 45 50.77400	124 06 40.56007	211.126
HOH_03	47 46 13.43625	124 20 12.49422	120.927
HOH_04*	47 48 25.10124	124 06 04.72567	103.347
HOH_05*	47 50 58.31806	124 17 06.70564	161.811
HOH_06	47 48 29.88648	-123 59 30.05375	194.895
USDOT_MINNIE	47 49 00.34169	-124 09 45.51533	61.924

*Used only for RTK during the upper watershed acquisition.

To correct the continuous onboard measurements of the aircraft position recorded throughout the missions, WSI concurrently conducted multiple static Global Navigation Satellite System (GNSS) ground surveys (1 Hz recording frequency) over each monument. After the airborne survey, the static GPS data were triangulated with nearby Continuously Operating Reference Stations (CORS) using the Online Positioning User Service (OPUS[1]) for precise positioning. Multiple independent sessions over the same monument were processed to confirm antenna height measurements and to refine position accuracy.

[1] OPUS is a free service provided by the National Geodetic Survey to process corrected monument positions. http://www.ngs.noaa.gov/OPUS.

Monuments were established according to the national standard for geodetic control networks, as specified in the Federal Geographic Data Committee (FGDC) Geospatial Positioning Accuracy Standards for geodetic networks.[2] This standard provides guidelines for classification of monument quality at the 95% confidence interval as a basis for comparing the quality of one control network to another. The monument rating for this project can be seen in Table 4.

Table 4: Federal Geographic Data Committee monument rating

Direction	Rating
St Dev $_{NE}$:	0.050 m
St Dev $_{z}$:	0.050 m

For the Hoh River Basin LiDAR project, the monument positions contributed no more than 5 cm of horizontal and vertical error to the final RTK and LiDAR positions, with 95% confidence.

RTK Surveys

For the real time kinematic (RTK) check point data collection, a Trimble R7 base unit was positioned at a nearby monument to broadcast a kinematic correction to a roving Trimble R8 GNSS receiver. All RTK measurements were made during periods with a Position Dilution of Precision (PDOP) of ≤ 3.0 with at least six satellites in view of the stationary and roving receivers. When collecting RTK data, the rover would record data while stationary for five seconds, then calculate the pseudorange position using at least three one-second epochs. Relative errors for the position must be less than 1.5 cm horizontal and 2.0 cm vertical in order to be accepted. See Table 5 for Trimble unit specifications.

RTK positions were collected on paved roads and other hard surface locations such as gravel or stable dirt roads that also had good satellite visibility. RTK measurements were not taken on highly reflective surfaces such as center line stripes or lane markings on roads due to the increased noise seen in the laser returns over these surfaces. The distribution of RTK points depended on ground access constraints and may not be equitably distributed throughout the study area. See Figure 2 for the distribution of RTK in this project.

Table 5: Trimble equipment identification

Receiver Model	Antenna	OPUS Antenna ID	Use
Trimble R7 GNSS	Zephyr GNSS Geodetic Model 2	TRM57971.00	Static
Trimble R8	Integrated Antenna R8 Model 2	TRM_R8_GNSS	RTK

[2] Federal Geographic Data Committee, Geospatial Positioning Accuracy Standards (FGDC-STD-007.2-1998). Part 2: Standards for Geodetic Networks, Table 2.1, page 2-3. http://www.fgdc.gov/standards/projects/FGDC-standards-projects/accuracy/part2/chapter2

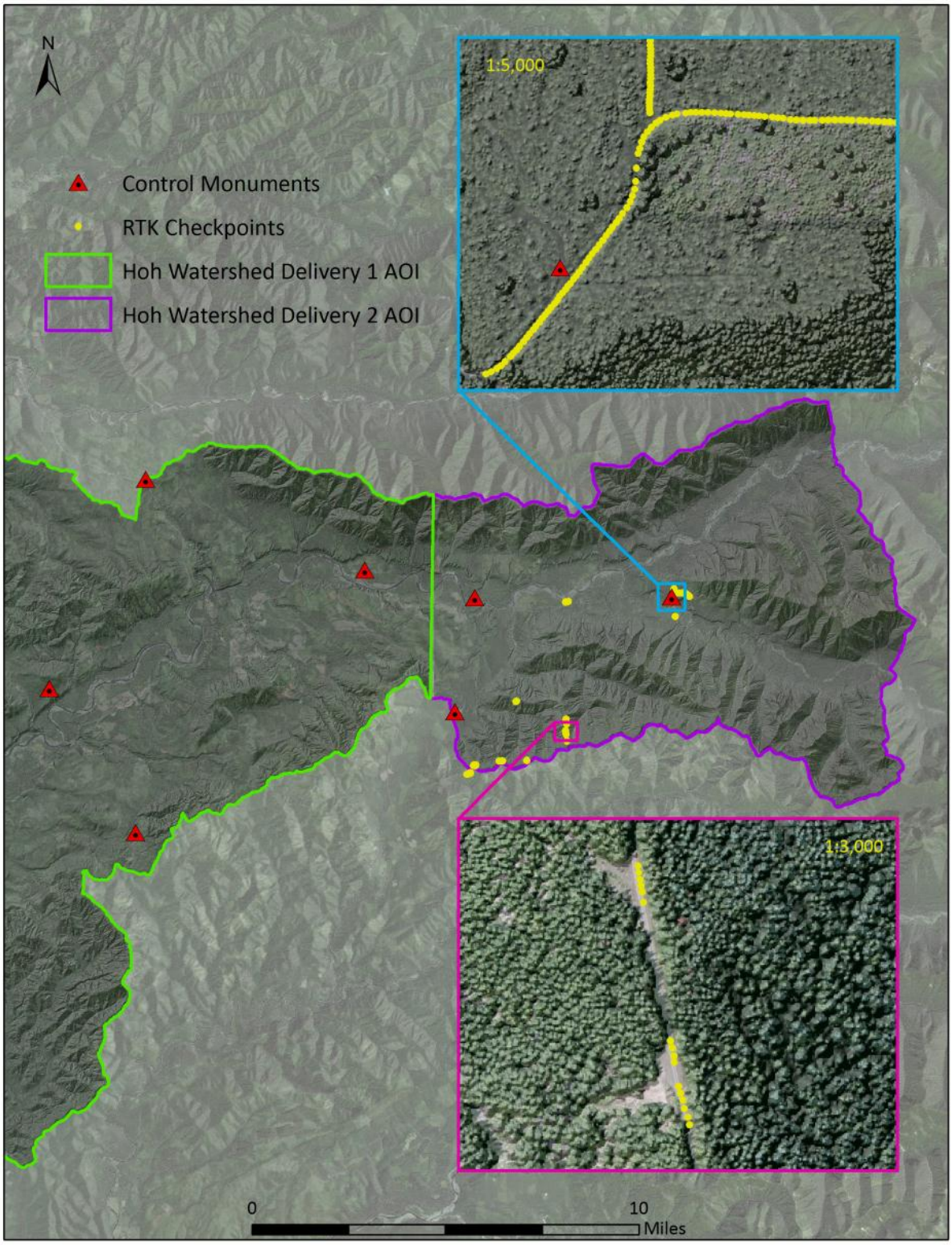

Figure 2: Basestation and RTK checkpoint location map

Airborne Survey

LiDAR

The LiDAR survey was accomplished with Leica ALS50 Phase II and ALS60 systems. Table 6 summarizes the settings used to yield an average pulse density of ≥ 8 pulses/m^2 over the Hoh River terrain. It is not uncommon for some types of surfaces (e.g. dense vegetation or water) to return fewer pulses to the LiDAR sensor than the laser originally emitted. These discrepancies between native and delivered density will vary depending on terrain, land cover, and the prevalence of water bodies.

Table 6: LiDAR specifications and survey settings

LiDAR Survey Settings & Specifications				
Dates	10/06-07/2012 10/10/2012	03/31/2013 04/01/2013	06/29-30/2013	07/24/2013
Sensor	Leica ALS50	Leica ALS60	Leica ALS50	Leica ALS50
Survey Altitude (AGL)	900 m	900 m	900 m	1,000 m
Target Pulse Rate	93-107.8 kHz	93-107.8 kHz	93-107.8 kHz	85-99.2 kHz
Sensor Configuration	SPiA*	SPiA*	SPiA*	SPiA*
Laser Pulse Diameter	21 cm	21 cm	21 cm	23 cm
Mirror Scan Rate	54.0 Hz	63.3 Hz	54.0 Hz	52.2 Hz
Field of View	28°	28°	28°	30°
GPS Baselines	≤13 nm	≤13 nm	≤13 nm	≤13 nm
GPS PDOP	≤3.0	≤3.0	≤3.0	≤3.0
GPS Satellite Constellation	≥6	≥6	≥6	≥6
Maximum Returns	4	4	4	4
Intensity	8-bit	8-bit	8-bit	8-bit
Accuracy	$RMSE_Z$ ≤ 15 cm	$RMSE_Z$ ≤ 15 cm	$RMSE_Z$ ≤ 15 cm	$RMSE_Z$ ≤ 15 cm

** Single Pulse in Air*

To reduce laser shadowing and increase surface laser painting, all areas were surveyed with an opposing flight line side-lap of ≥50% (≥100% overlap). The Leica laser systems record up to four range measurements (returns) per pulse. All discernible laser returns were processed for the output dataset.

To accurately solve for laser point position (geographic coordinates x, y, z), the positional coordinates of the airborne sensor and the attitude of the aircraft were recorded continuously throughout the LiDAR data collection mission. Position of the aircraft was measured twice per second (2 Hz) by an onboard differential GPS unit. Aircraft attitude was measured 200 times per second (200 Hz) as pitch, roll, and yaw (heading) from an onboard inertial measurement unit (IMU). To allow for post-processing correction and calibration, aircraft/sensor position and attitude data are indexed by GPS time.

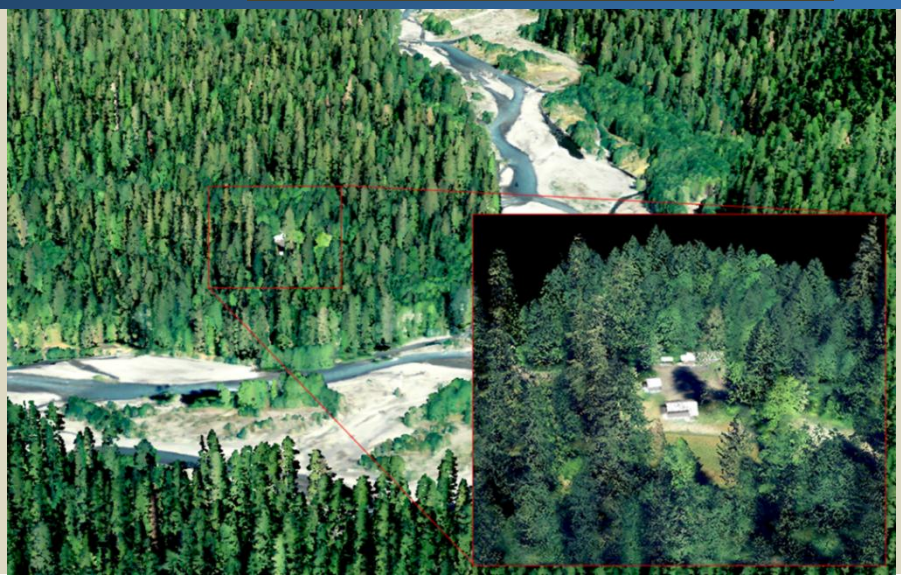

View of the Hoh Rain Forest Center. Images created from the LIDAR point cloud with RGB values assigned with 2011 NAIP imagery.

LiDAR Data

Upon the LiDAR data's arrival to the office, WSI processing staff initiates a suite of automated and manual techniques to process the data into the requested deliverables. Processing tasks include GPS control computations, smoothed best estimate trajectory (SBET) calculations, kinematic corrections, calculation of laser point position, calibration for optimal relative and absolute accuracy, and classification of ground and non-ground points (Table 7). Processing methodologies are tailored for the landscape and intended application of the point data. A full description of these tasks can be found in Table 8.

Table 7: ASPRS LAS classification standards applied to the Hoh River dataset

Classification Number	Classification Name	Classification Description
1	Default/ Unclassified	Laser returns that are not included in the ground class and not dismissed as Noise or Withheld points
2	Ground	Ground that is determined by a number of automated and manual cleaning algorithms to determine the best ground model the data can support
4	Low Vegetation	Any vegetation within 0.75 ft of the ground surface
5	Medium Vegetation	Vegetation more than 0.75 ft above ground
6	Building	Man Made features
7	Low Points	Noise (i.e. pits, birds, etc.)
9	Water	Water
10	Ignored Ground	Ground points proximate to breaklines, ignored for breakline enforcement in the hydroflattened and enforced bare earth model
11	Withheld	Points with intensity values at the far ends of the intensity range (0 or 255)
15	Snow	Snow accumulation on a small segment of dirt road during the 2012 acquisition. Overlapping flightlines from the 2013 acquisition captured the true road surface, thus the snow classification of the 2012 data

Table 8: LiDAR processing workflow

LiDAR Processing Step	Software Used
Resolve kinematic corrections for aircraft position data using kinematic aircraft GPS and static ground GPS data.	Waypoint GPS v.8.3 Trimble Business Center v.3.00 Geographic Calculator 2013
Develop a smoothed best estimate of trajectory (SBET) file that blends post-processed aircraft position with attitude data. Sensor head position and attitude are calculated throughout the survey. The SBET data are used extensively for laser point processing.	IPAS TC v.3.1
Calculate laser point position by associating SBET position to each laser point return time, scan angle, intensity, etc. Create raw laser point cloud data for the entire survey in *.las (ASPRS v. 1.2) format. Data are converted to orthometric elevations (NAVD88) by applying a Geoid12 correction.	ALS Post Processing Software v.2.74
Import raw laser points into manageable blocks (less than 500 MB) to perform manual relative accuracy calibration and filter erroneous points. Ground points are then classified for individual flight lines (to be used for relative accuracy testing and calibration).	TerraScan v.13.008
Using ground classified points per each flight line, the relative accuracy is tested. Automated line-to-line calibrations are then performed for system attitude parameters (pitch, roll, heading), mirror flex (scale) and GPS/IMU drift. Calibrations are calculated on ground classified points from paired flight lines and results are applied to all points in a flight line. Every flight line is used for relative accuracy calibration.	TerraMatch v.13.002
Classify resulting data to ground and other client designated ASPRS classifications (Table 7). Assess statistical absolute accuracy via direct comparisons of ground classified points to ground RTK survey data.	TerraScan v.13.008 TerraModeler v.13.002
Generate bare earth models as triangulated surfaces. Highest hit models were created as a surface expression of all classified points (excluding the noise and withheld classes). All surface models were exported as ESRI grids at a 3-foot pixel resolution.	TerraScan v.13.008 ArcMap v. 10.1 TerraModeler v.13.002

Feature Extraction

Hydro-flattening

WSI created hydro-flattening breaklines for the Hoh River to flatten water surfaces greater than ~100 feet in width. The hydro-flattening process eliminates artifacts in the digital terrain model caused by both increased variability in ranges and dropouts in laser returns due to the low reflectivity of water. The water's edge was detected using an algorithm which weights LiDAR-derived slopes, intensities, and return densities to detect the water's edge. Elevations were assigned to the water's edge through neighborhood statistics identifying the lowest LiDAR return from the water surface. Lakes were assigned a consistent elevation for an entire polygon while rivers were assigned consistent elevations on opposing banks and smoothed to ensure downstream flow through the entire river channel. These breaklines were incorporated into the hydro-flattened DEM by enforcing triangle edges (adjacent to the breakline) to the elevation values derived from the breakline. This implementation corrected interpolation along the hard edge. Water surfaces were obtained from a TIN of the 3-D water edge breaklines resulting in the final hydroflattened model (Figure 3).

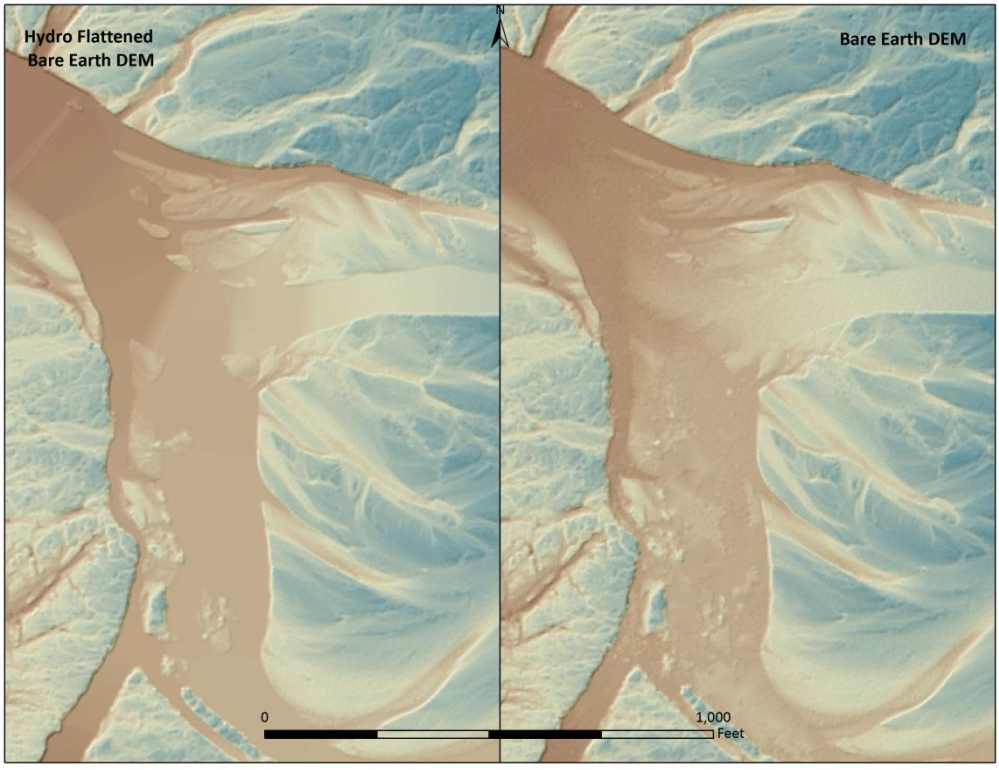

Figure 3: Example of hydro-flattening in the Hoh River LiDAR dataset

Hydro Enforcement and Stream Network

The stream network for the Hoh AOI was generated from the LiDAR-derived bare earth DEMs using ArcHydro 2.0. An initial network was generated by filling all sinks (depressions) in the model and identifying all paths of flow with an accumulation threshold of at least 2.5 acres. This initial stream network was inspected for artificial obstructions to the flow (i.e. culverts beneath roads that allow flow but are not reflected in the normal bare earth model). Small hydro-enforcement breaklines were then incorporated into the bare earth model at obstruction locations to enforce the appropriate flow path (Figure 4). ArcHydro was then re-run on the resulting hydro-enforced bare earth model. The resulting stream network of all flow paths with a flow accumulation of at least 2.5 acres was then manually edited to remove stream segments where no channelization was evident in the ground model. The final stream network (Figure 5) has been checked for topological consistency and compared to the National Hydrography dataset.

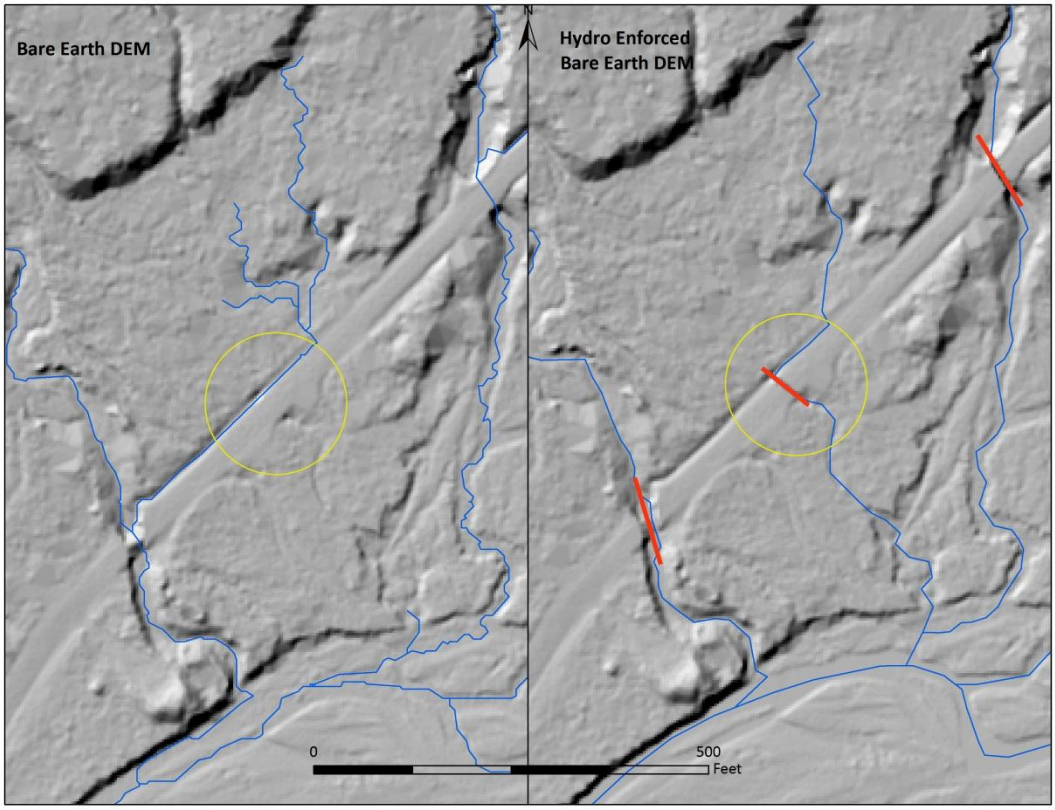

Figure 4: ArcHydro generated stream network displayed over a bare earth DEM and a hydro-enforced bare earth DEM. The red lines indicate areas on the DEM that were 'enforced' to correct erroneous flow paths.

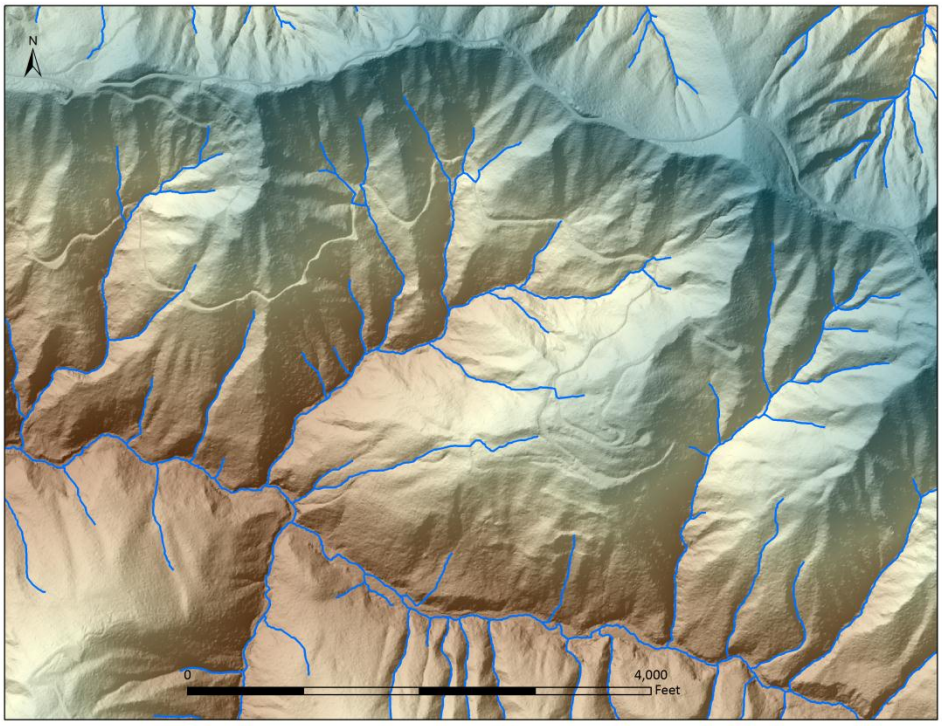

Figure 5: ArcHydro generated stream network

Contours

Contour generation from LiDAR point data requires a thinning operation in order to reduce contour sinuosity. The thinning operation reduces point density where topographic change is minimal (flat surfaces) while preserving resolution where topographic change is present. These model key points are selected from the ground model every 20 feet with the spacing decreased in regions with high surface curvature (Z tolerance of 0.15 feet). Generation of model key points eliminates redundant detail in terrain representation, particularly in areas of low relief, and provides for a more manageable dataset. Contours are produced through TerraModeler by interpolating between the model key points at even elevation increments.

Contour lines are then intersected with ground point density rasters and a confidence level attribute is added to each contour line. A confidence code of '0' is used to identify contours in areas of high point density while a confidence code of '1' is assigned to contours crossing areas with lower ground point densities. Areas with low ground point density are commonly beneath buildings and bridges, in locations with dense vegetation, over water, and in other areas where laser penetration to the ground surface is impeded (Figure 6).

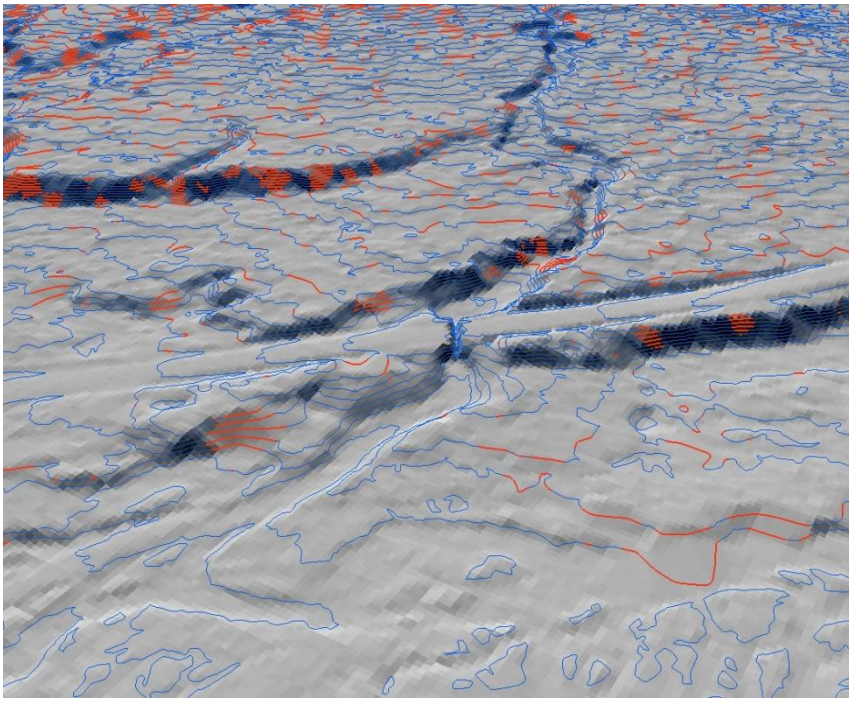

Figure 6: Contours draped over the Hoh River bare earth elevation model. Blue contours represent high confidence while the red contours represent low confidence.

Building and Bridge Footprints

Building and bridge classification was performed through a combination of automated algorithms and manual classification. Typically, manual editing was necessary where dense canopy was immediately proximate to features. Once classification was complete, automated routines were used generate the polygon shapefile representing building and bridge footprints.

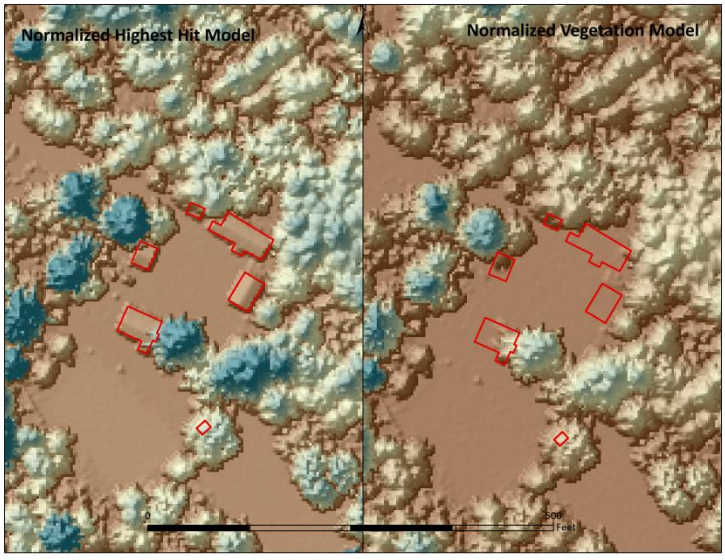

Figure 7: Sample image of building and bridge footprints in the Hoh River dataset

View looking north at the ridgeline above the Hoh Rain Forest. Left image created from gridded ground-classified LiDAR points colored by elevation. Right image created from the point cloud with RGB values assigned with 2011 NAIP imagery.

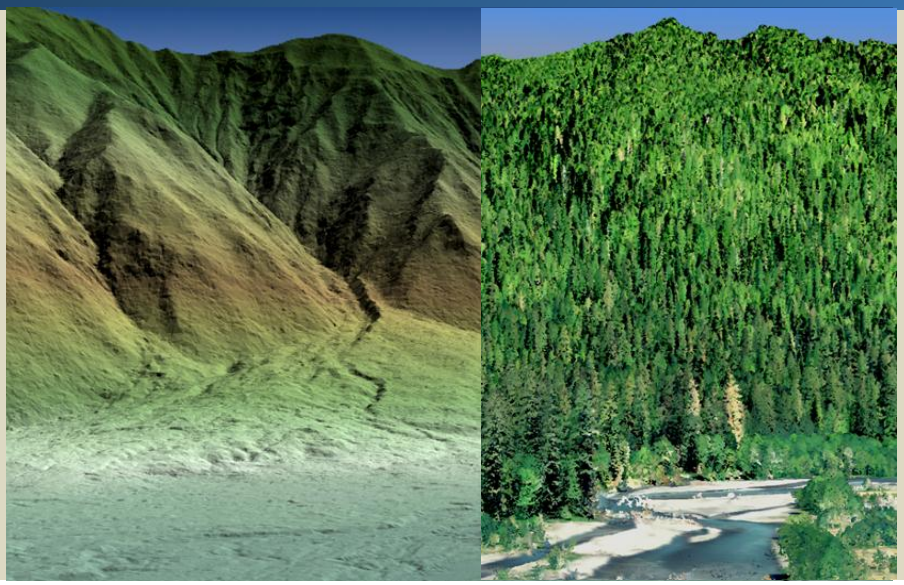

LiDAR Density

The sensor is set to acquire a native density of 8 points/m^2. Depending on the nature of the terrain, the first returned echo will be the highest hit surface. In vegetated areas, the first return surface will represent the top of the canopy, while in clearings or on paved roads, the first return surface will represent the ground. The ground density differs from the first return density due to the fact that in vegetated areas, fewer returns may penetrate the canopy. The ground classification is generally determined by first echo returns in non-vegetated areas combined with last echo returns in vegetated areas. The pulse density distribution will vary within the study area due to laser scan pattern and flight conditions. Additionally, some types of surfaces (i.e. breaks in terrain, water, steep slopes) may return fewer pulses to the sensor than originally emitted by the laser.

The average first return density for the cumulative LiDAR dataset for the Hoh River (D1 and D2) was 0.89 points/ft^2 (9.54 points/m^2) while the average ground classified density was 0.07 points/ft^2 (0.745 points/m^2) (Table 9). Low ground densities are a direct result of the dense rainforest vegetation in the drainage. The statistical distribution of cumulative first returns (Figure 8) and classified ground points (Figure 9) are portrayed below. The spatial distribution of average first return densities by delivery can be seen in Figure 10 and Figure 11, with ground point densities shown in Figure 12 and Figure 13.

Table 9: Average LiDAR point densities

Classification	Cumulative (D1 & D2)	Delivery 1	Delivery 2
First Return	0.87 points/ft^2 9.54 points/m^2	0.78 points/ft^2 8.40 points/m^2	1.10 points/ft^2 11.86 points/m^2
Ground Classified	0.07points/ft^2 0.75 points/m^2	0.07 points/ft^2 0.75 points/m^2	0.07 points/ft^2 0.74 points/m^2

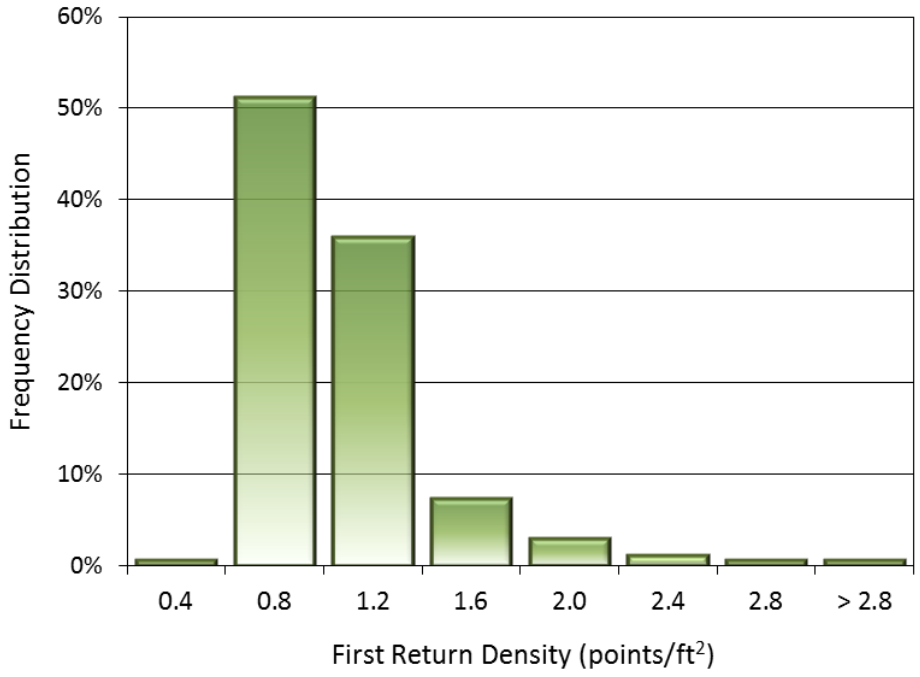

Figure 8: Frequency distribution of first return densities (native densities) of the gridded study area (cumulative)

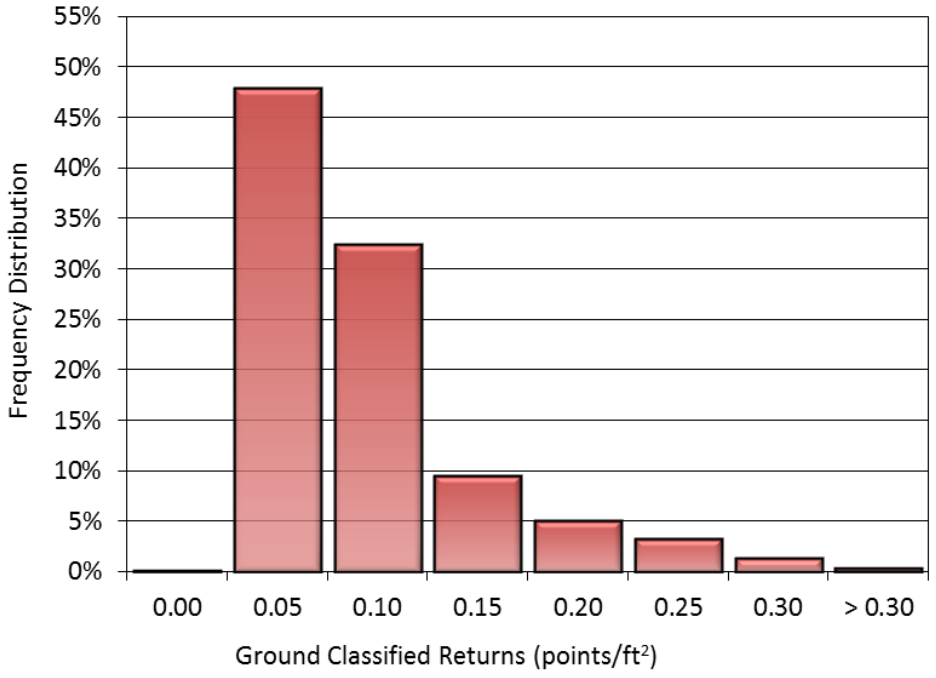

Figure 9: Frequency distribution of ground return densities of the gridded study area (cumulative)

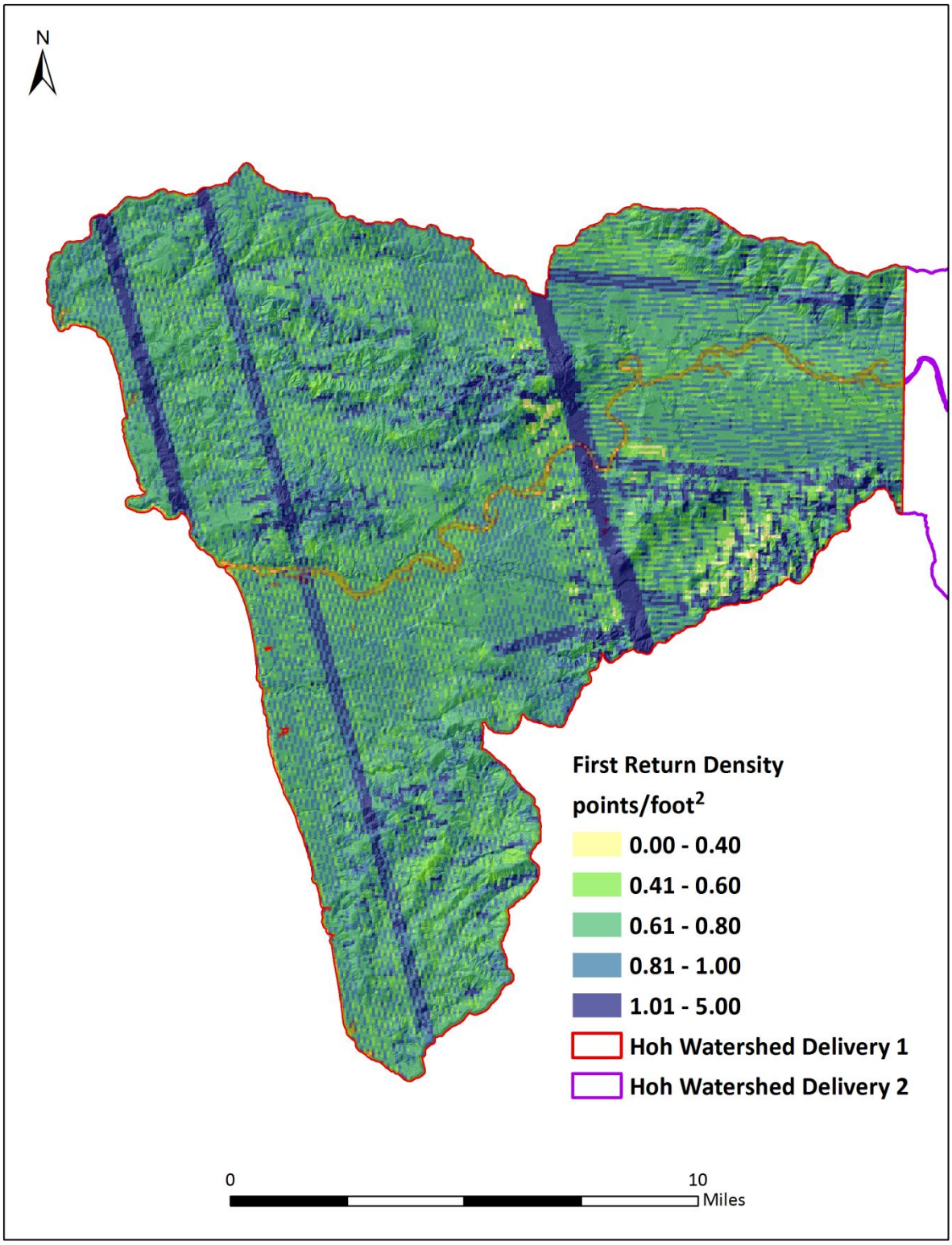

Figure 10: Native density map for the Hoh River site – Delivery 1 (100mx100m cells)

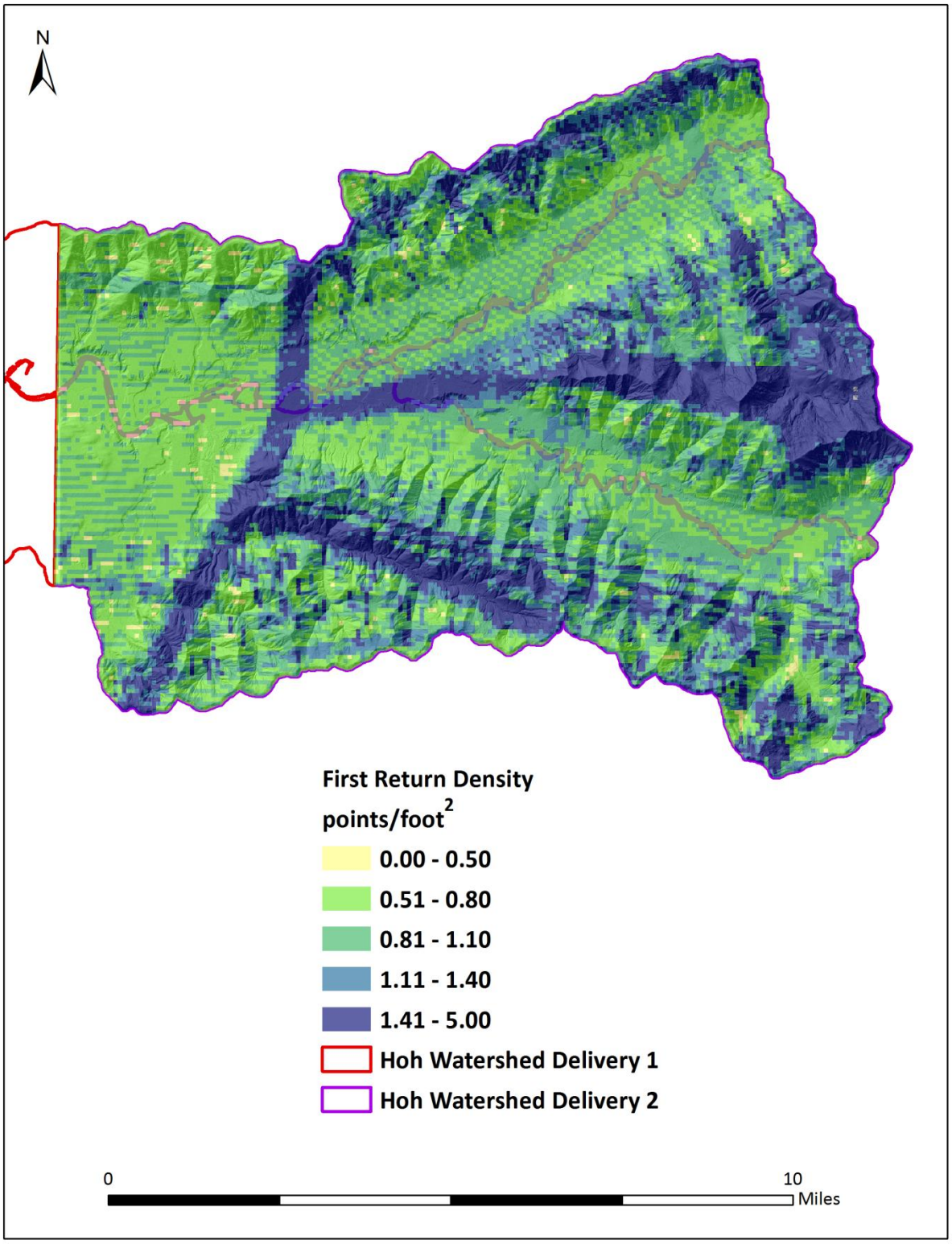

Figure 11: Native density map for the Hoh River site – Delivery 2 (100mx100m cells)

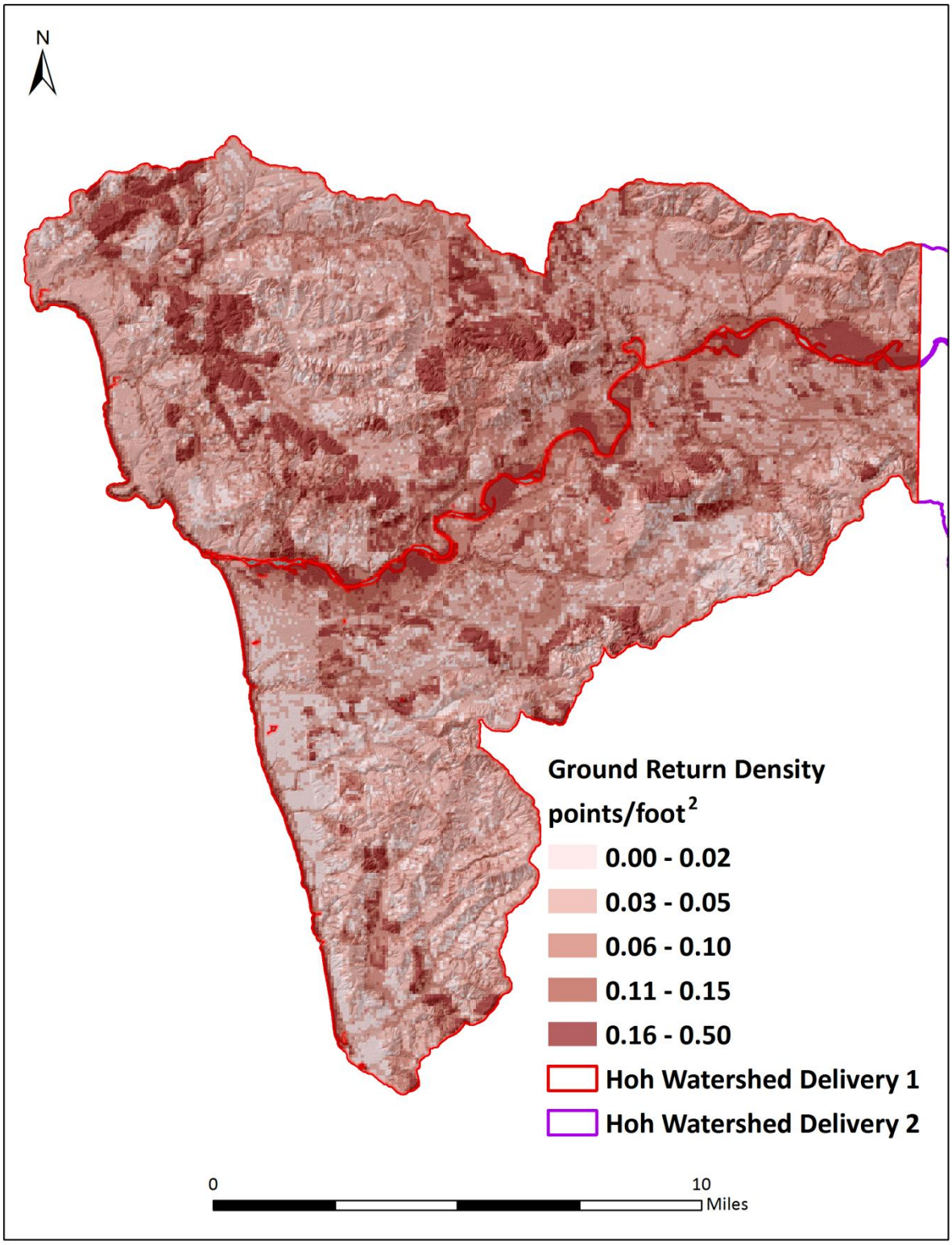

Figure 12: Ground density map for the Hoh River site- Delivery 1 (100mx100m cells)

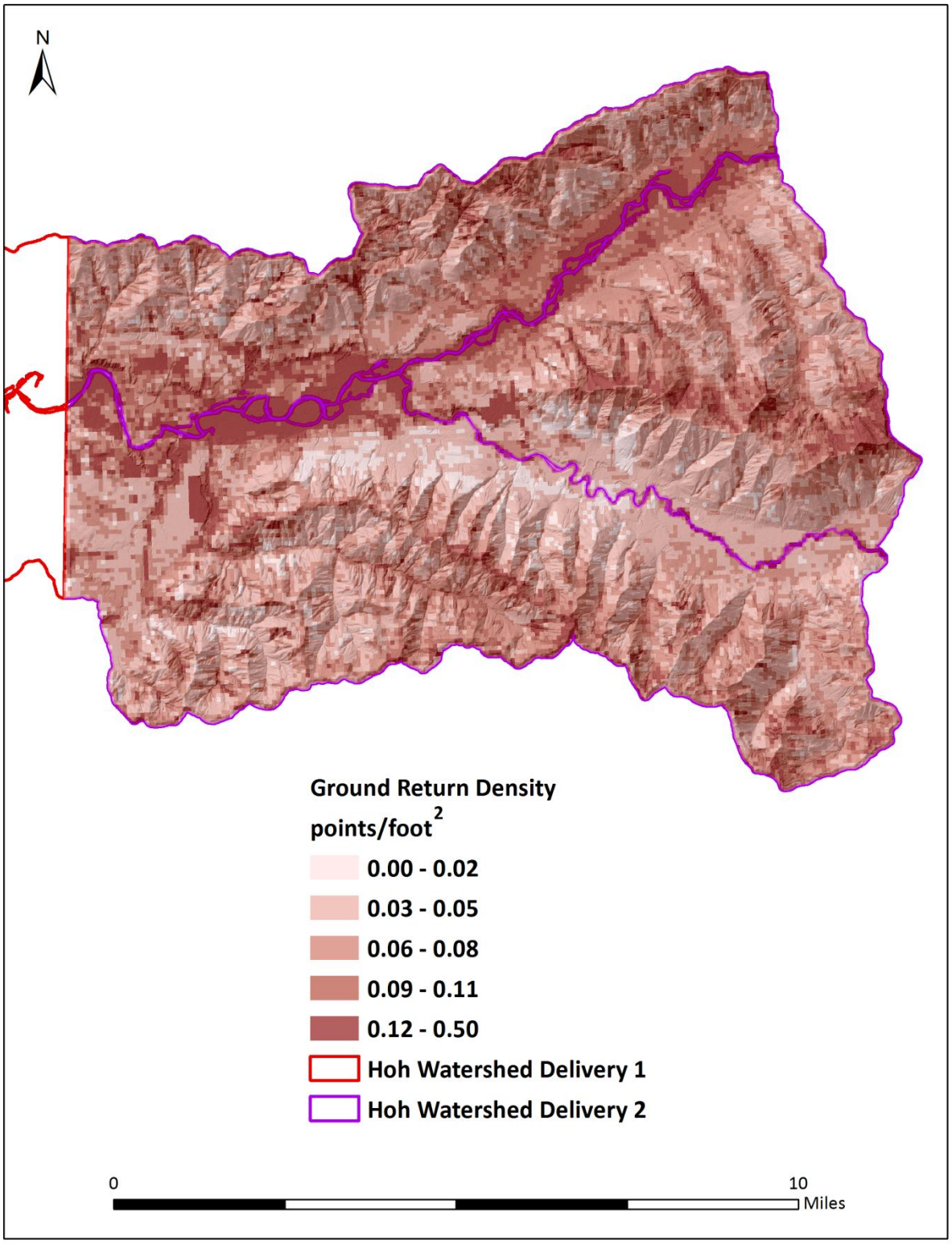

Figure 13: Ground density map for the Hoh River site- Delivery 2 (100mx100m cells)

LiDAR Accuracy Assessments

The accuracy of the LiDAR data collection can be described in terms of absolute accuracy (the consistency of the data with external data sources) and relative accuracy (the consistency of the dataset with itself). See Appendix A for further information on sources of error and operational measures used to improve relative accuracy.

LiDAR Absolute Accuracy

Vertical absolute accuracy was primarily assessed from RTK ground check point (GCP) data collected on open, bare earth surfaces with level slope (<20°). Fundamental Vertical Accuracy (FVA) reporting is designed to meet guidelines presented in the FGDC National Standard for Spatial Data Accuracy for horizontal accuracy[3]. FVA compares known RTK ground survey check points to the triangulated ground surface generated by the LiDAR points. FVA is a measure of the accuracy of LiDAR point data in open areas where the LiDAR system has a "very high probability" of measuring the ground surface and is evaluated at the 95% confidence interval (1.96 σ).

Absolute accuracy is described as the mean and standard deviation (sigma σ) of divergence of the ground surface model from ground survey point coordinates. These statistics assume the error for x, y, and z is normally distributed, and therefore the skew and kurtosis of distributions are also considered when evaluating error statistics. For the Hoh River survey, 2740 RTK points were collected in total resulting in an average accuracy of -0.023 feet (Table 10, Figure 14).

Table 10: Absolute accuracies for the Hoh River LiDAR dataset

	Units	Cumulative	Delivery 1	Delivery 2
Sample	*points*	2740	2087	653
Average	*ft*	-0.089	-.089	-0.091
	m	-0.027	-0.027	-0.028
Median	*ft*	-0.082	-0.079	-0.092
	m	-0.025	-0.024	-0.028
RMSE	*ft*	0.141	0.143	0.131
	m	0.043	0.044	0.040
Standard Deviation (1σ)	*ft*	0.109	0.113	0.094
	m	0.033	0.034	0.029
1.96σ	*ft*	0.213	0.221	0.184
	m	0.065	0.067	0.056

[3] Federal Geographic Data Committee, Geospatial Positioning Accuracy Standards (FGDC-STD-007.3-1998). Part 3: National Standard for Spatial Data Accuracy. http://www.fgdc.gov/standards/projects/FGDC-standards-projects/accuracy/part3/chapter3

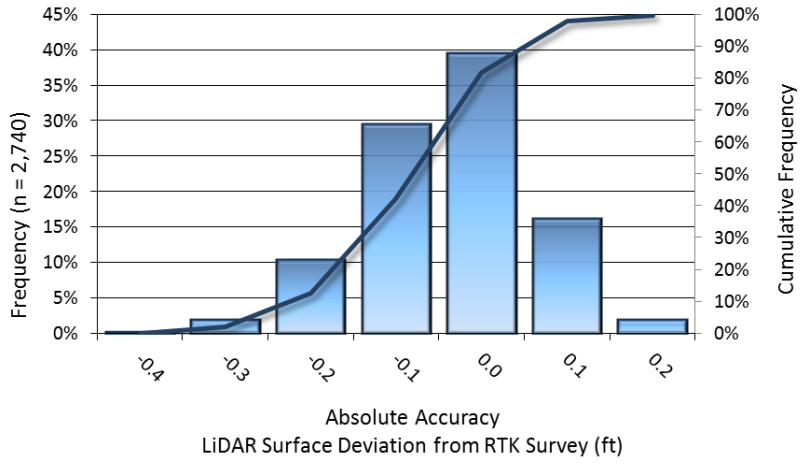

Figure 14: Frequency histogram for LiDAR surface deviation from RTK values - Cumulative

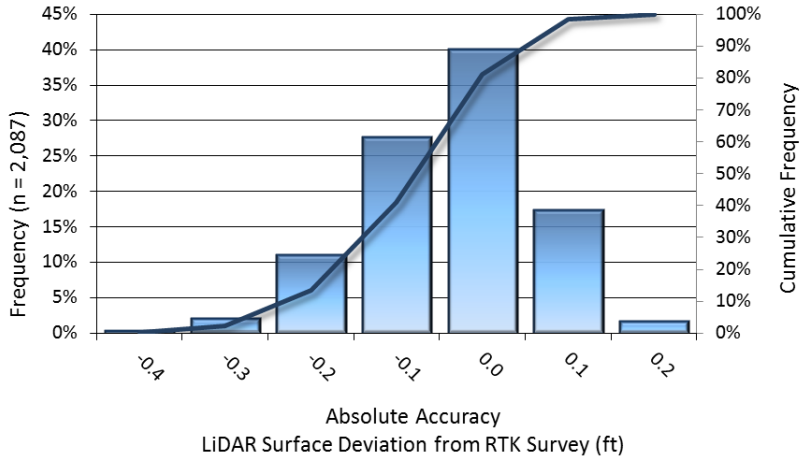

Figure 155: Frequency histogram for LiDAR surface deviation from RTK values – Delivery 1

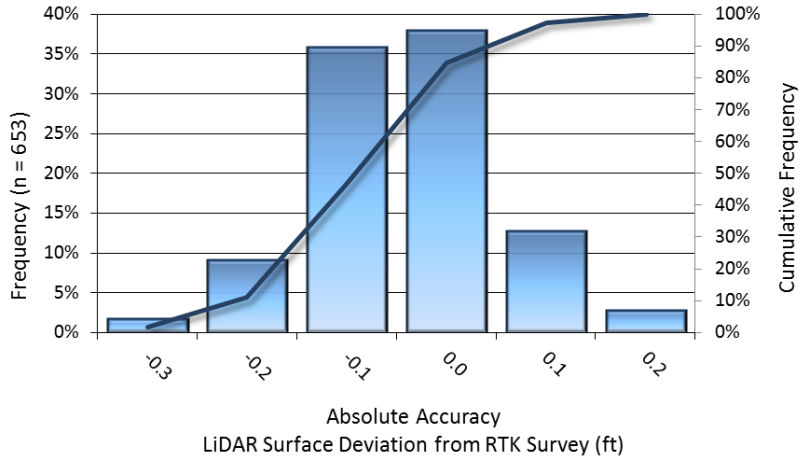

Figure 166: Frequency histogram for LiDAR surface deviation from RTK values – Delivery 2

LiDAR Vertical Relative Accuracy

Relative vertical accuracy refers to the internal consistency of the data set as a whole: the ability to place an object in the same location given multiple flight lines, GPS conditions, and aircraft attitudes. When the LiDAR system is well calibrated, the swath-to-swath vertical divergence is low (<0.10 meters). The relative vertical accuracy is computed by comparing the ground surface model of each individual flight line with its neighbors in overlapping regions. The average (mean) line to line relative vertical accuracy for the Hoh River was 0.214 feet (Table 11, Figure 177).

Table 11: Relative accuracies for the Hoh River LiDAR dataset

	Units	Cumulative	Delivery 1	Delivery 2
Sample	*surfaces*	608	304	304
Average	*ft*	0.214	0.205	0.240
	m	0.065	0.062	0.073
Median	*ft*	0.228	0.212	0.248
	m	0.070	0.065	0.076
RMSE	*ft*	0.269	0.264	0.274
	m	0.082	0.080	0.084
Standard Deviation (1σ)	*ft*	0.097	0.094	0.100
	m	0.030	0.029	0.030
1.96σ	*ft*	0.190	0.184	0.195
	m	0.058	0.056	0.060

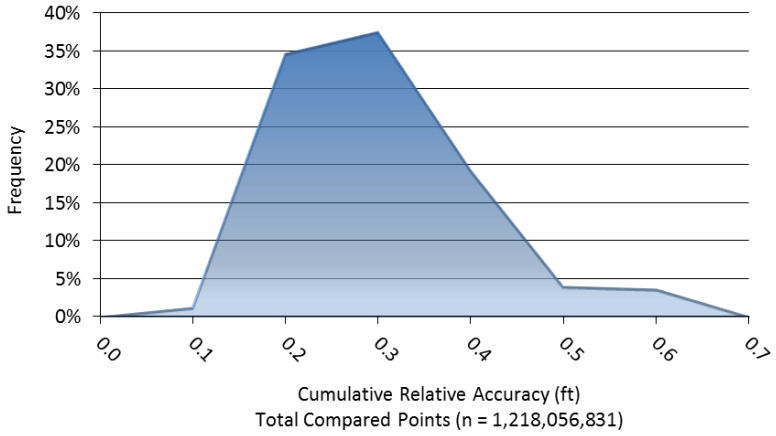

Figure 177: Frequency plot for relative vertical accuracy between flight lines – Cumulative

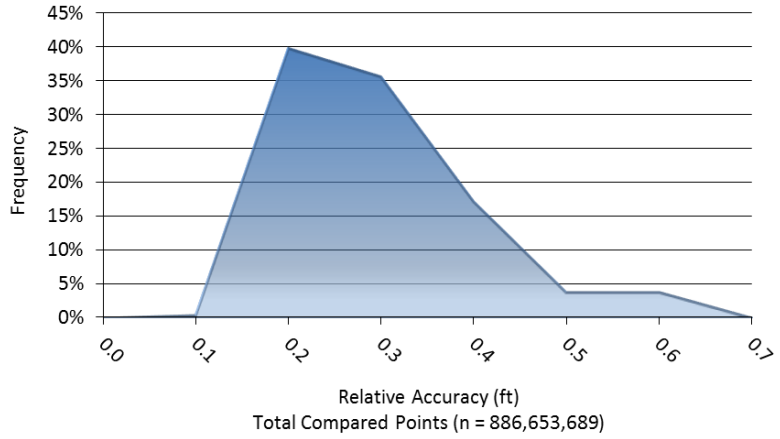

Figure 188: Frequency plot for relative vertical accuracy between flight lines – Delivery 1

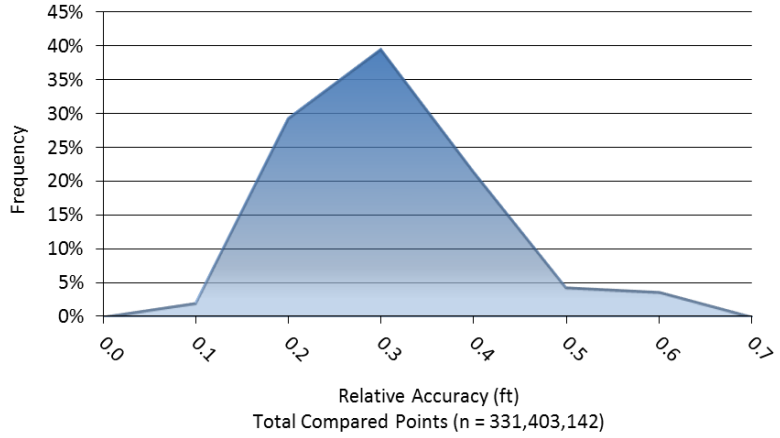

Figure 199: Frequency plot for relative vertical accuracy between flight lines – Delivery 2

CERTIFICATIONS

Watershed Sciences provided LiDAR services for the Hoh River Watershed study area as described in this report.

I, Russ Faux, have reviewed the attached report for completeness and hereby state that it is a complete and accurate report of this project.

Russ Faux
Principal
WSI

I, Christopher W. Yotter-Brown, being first duly sworn, say that as described in the Ground Survey subsection of the Acquisition section of this report was completed by me or under my direct supervision and was completed using commonly accepted standard practices. Accuracy statistics shown in the Accuracy Section have been reviewed by me to meet National Standard for Spatial Data Accuracy.

8/29/2013

Christopher W. Yotter-Brown, PLS Oregon & Washington
WSI
Portland, OR 97204

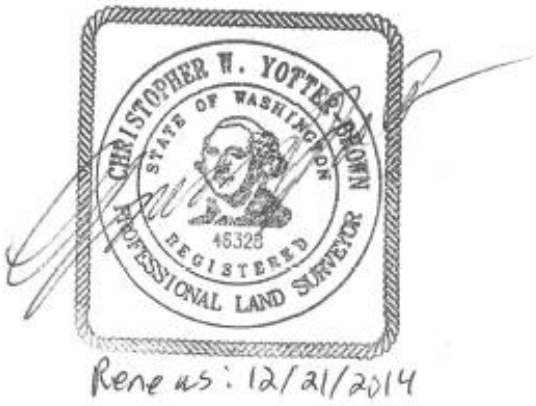

Renews: 12/21/2014

Figure 20: View looking southwest at Hoh River near the Hoh Rain Forest Center. Top image created from gridded ground-classified LiDAR points colored by elevation. Bottom image created from the LIDAR point cloud with RGB values assigned with 2011 NAIP imagery.

GLOSSARY

1-sigma (σ) Absolute Deviation: Value for which the data are within one standard deviation (approximately 68th percentile) of a normally distributed data set.

1.96-sigma (σ) Absolute Deviation: Value for which the data are within two standard deviations (approximately 95th percentile) of a normally distributed data set.

Accuracy: The statistical comparison between known (surveyed) points and laser points. Typically measured as the standard deviation (sigma σ) and root mean square error (RMSE).

> **Absolute Accuracy:** The vertical accuracy of LiDAR data is described as the mean and standard deviation (sigma σ) of divergence of LiDAR point coordinates from RTK ground survey point coordinates. To provide a sense of the model predictive power of the dataset, the root mean square error (RMSE) for vertical accuracy is also provided. These statistics assume the error distributions for x, y, and z are normally distributed, thus we also consider the skew and kurtosis of distributions when evaluating error statistics.
>
> **Relative Accuracy:** Relative accuracy refers to the internal consistency of the data set - the ability to place a laser point in the same location over multiple flight lines, GPS conditions, and aircraft attitudes. Affected by system attitude offsets, scale, and GPS/IMU drift, internal consistency is measured as the divergence between points from different flight lines within an overlapping area. Divergence is most apparent when flight lines are opposing. When the LiDAR system is well calibrated, the line-to-line divergence is low (<10 cm).
>
> **Root Mean Square Error (RMSE):** A statistic used to approximate the difference between real-world points and the LiDAR points. It is calculated by squaring all the values, then taking the average of the squares and taking the square root of the average.

Data Density: A common measure of LiDAR resolution, measured as points per square meter.

DTM / DEM: These often-interchanged terms refer to models made from laser points. The digital elevation model (DEM) refers to all surfaces, including bare ground and vegetation, while the digital terrain model (DTM) refers only to those points classified as ground.

Intensity Values: The peak power ratio of the laser return to the emitted laser. It is a function of surface reflectivity.

Laser Noise: For any given target, laser noise is the breadth of the data cloud per laser return (i.e., last, first, etc.). Lower intensity surfaces (roads, rooftops, still/calm water) experience higher laser noise.

Nadir: A single point or locus of points on the surface of the earth directly below a sensor as it progresses along its flight line.

Overlap: The area shared between flight lines, typically measured in percent; 100% overlap is essential to ensure complete coverage and reduce laser shadows.

Pulse Rate (PR): The rate at which laser pulses are emitted from the sensor; typically measured as thousands of pulses per second (kHz).

Pulse Returns: For every laser pulse emitted, the Leica ALS 60 system can record *up to four* wave forms reflected back to the sensor. Portions of the wave form that return earliest are the highest element in multi-tiered surfaces such as vegetation. Portions of the wave form that return last are the lowest element in multi-tiered surfaces.

Real-Time Kinematic (RTK) Survey: GPS surveying is conducted with a GPS base station deployed over a known monument with a radio connection to a GPS rover. Both the base station and rover receive differential GPS data and the baseline correction is solved between the two. This type of ground survey is accurate to 1.5 cm or less.

Scan Angle: The angle from nadir to the edge of the scan, measured in degrees. Laser point accuracy typically decreases as scan angles increase.

Spot Spacing: Also a measure of LiDAR resolution, measured as the average distance between laser points.

Relative Accuracy Calibration Methodology:

Manual System Calibration: Calibration procedures for each mission require solving geometric relationships that relate measured swath-to-swath deviations to misalignments of system attitude parameters. Corrected scale, pitch, roll and heading offsets were calculated and applied to resolve misalignments. The raw divergence between lines was computed after the manual calibration was completed and reported for each survey area.

Automated Attitude Calibration: All data were tested and calibrated using TerraMatch automated sampling routines. Ground points were classified for each individual flight line and used for line-to-line testing. System misalignment offsets (pitch, roll and heading) and scale were solved for each individual mission and applied to respective mission datasets. The data from each mission were then blended when imported together to form the entire area of interest.

Automated Z Calibration: Ground points per line were used to calculate the vertical divergence between lines caused by vertical GPS drift. Automated Z calibration was the final step employed for relative accuracy calibration.

LiDAR accuracy error sources and solutions:

Type of Error	Source	Post Processing Solution
GPS (Static/Kinematic)	Long Base Lines	None
	Poor Satellite Constellation	None
	Poor Antenna Visibility	Reduce Visibility Mask
Relative Accuracy	Poor System Calibration	Recalibrate IMU and sensor offsets/settings
	Inaccurate System	None
Laser Noise	Poor Laser Timing	None
	Poor Laser Reception	None
	Poor Laser Power	None
	Irregular Laser Shape	None

Operational measures taken to improve relative accuracy:

Low Flight Altitude: Terrain following is employed to maintain a constant above ground level (AGL). Laser horizontal errors are a function of flight altitude above ground (i.e., ~ $1/3000^{th}$ AGL flight altitude).

Focus Laser Power at narrow beam footprint: A laser return must be received by the system above a power threshold to accurately record a measurement. The strength of the laser return is a function of laser emission power, laser footprint, flight altitude and the reflectivity of the target. While surface reflectivity cannot be controlled, laser power can be increased and low flight altitudes can be maintained.

Reduced Scan Angle: Edge-of-scan data can become inaccurate. The scan angle was reduced to a maximum of $\pm 15^{\circ}$ from nadir, creating a narrow swath width and greatly reducing laser shadows from trees and buildings.

Quality GPS: Flights took place during optimal GPS conditions (e.g., 6 or more satellites and PDOP [Position Dilution of Precision] less than 3.0). Before each flight, the PDOP was determined for the survey day. During all flight times, a dual frequency DGPS base station recording at 1–second epochs was utilized and a maximum baseline length between the aircraft and the control points was less than 19 km (11.5 miles) at all times.

Ground Survey: Ground survey point accuracy (i.e. <1.5 cm RMSE) occurs during optimal PDOP ranges and targets a minimal baseline distance of 4 miles between GPS rover and base. Robust statistics are, in part, a function of sample size (n) and distribution. Ground survey RTK points are distributed to the extent possible throughout multiple flight lines and across the survey area.

50% Side-Lap (100% Overlap): Overlapping areas are optimized for relative accuracy testing. Laser shadowing is minimized to help increase target acquisition from multiple scan angles. Ideally, with a 50% side-lap, the most nadir portion of one flight line coincides with the edge (least nadir) portion of overlapping flight lines. A minimum of 50% side-lap with terrain-followed acquisition prevents data gaps.

Opposing Flight Lines: All overlapping flight lines are opposing. Pitch, roll and heading errors are amplified by a factor of two relative to the adjacent flight line(s), making misalignments easier to detect and resolve.